Environmental Science and Pollution Research (2021) 28:58050–58067
https://doi.org/10.1007/s11356-021-14528-8

RESEARCH ARTICLE

Detoxification and recovery after cadmium exposure in the freshwater crab *Sinopotamon henanense*

Zihan Xu[1] · Jing Liu[1] · Ermeng Wang[1] · Chenyun Zhao[1] · Xuelei Hu[2] · Ka Hou Chu[3] · Lan Wang[1]

Received: 26 November 2020 / Accepted: 18 May 2021 / Published online: 8 June 2021
© The Author(s), under exclusive licence to Springer-Verlag GmbH Germany, part of Springer Nature 2021

Abstract

Cadmium (Cd) is a common pollutant in the aquatic environment, which puts the health and safety of aquatic organisms and humans at risk. In the present study, the freshwater crab *Sinopotamon henanense* was exposed to Cd (0, 50, 100, and 500 $\mu g \cdot L^{-1}$) for 14 d (0–14th d), followed by 21 d (14–35th d) of depuration. The changes in Cd bioaccumulation, microstructure, biomacromolecules (polysaccharides, neutral lipids, DNA and total proteins), and biochemical parameters (SOD, CAT, GR, TrxR, MDA and AChE) in the gills and hepatopancreas were tested. The injured microstructure, activated antioxidant system, increased MDA, and inhibited AChE of the gills and hepatopancreas responded with progressive bioaccumulation of Cd. Meanwhile, the polysaccharides and neutral lipids in the hepatopancreas reduced and DNA synthesis enhanced. During depuration, more than 58.80 ± 8.53% and 13.84 ± 12.11% of Cd was excreted from the gills and hepatopancreas, respectively. Recovery of microstructure and biomacromolecules as well as alleviated oxidative damage and neurotoxicity were also found in these two organs. Additionally, based on PCA, I_{his}, GR and MDA were identified as the optimal biomarkers indicating the health status of crabs. In conclusion, *S. henanense* could resist Cd stress through antioxidant defence and self-detoxification.

Keywords Cadmium · *Sinopotamon henanense* · Detoxification · Recovery · Micromorphology · Biochemical parameters

Highlights
- Polysaccharides and neutral lipids of hepatocytes were susceptible to Cd stress.
- *S. henanense* resisted Cd through the antioxidant system during 21 d of depuration.
- The gills had a higher EC, better recovery capability than hepatopancreas.
- I_{his}, GR and MDA were suitable biomarkers showing the health status of *S. henanense*.

Responsible Editor: Bruno Nunes

✉ Lan Wang
lanwang@sxu.edu.cn

Zihan Xu
xzh960118@163.com

Jing Liu
494113059@qq.com

Ermeng Wang
Twodream920@qq.com

Chenyun Zhao
2414742105@qq.com

Xuelei Hu
xuelei.hu1987@gmail.com

Ka Hou Chu
kahouchu@cuhk.edu.hk

[1] School of Life Science, Shanxi University, Taiyuan 030006, Shanxi Province, China

[2] School of Biology and Food Engineering, Guangdong University of Education, Guangzhou 510303, Guangdong Province, China

[3] School of Life Sciences, The Chinese University of Hong Kong, Shatin, Hong Kong, SAR, China

Introduction

Cadmium (Cd) is a nonessential heavy metal (HM) with no physiological functions and high toxicity to cells and organs (Genchi et al. 2020). Cadmium pollution, especially in water, has become increasingly serious with its release from industry, agriculture and other human activities (Chiodi Boudet et al. 2015), and this problem has become a major issue to be addressed in several countries such as Australia (Chubaka et al. 2018), China (Zhao et al. 2018) and Uganda (Kasozi et al. 2019). Cadmium pollution in water does not only affect the life activities of the aquatic animals, cause structure and scale fluctuations of their populations, and destroy the balance of aquatic ecosystems but also damage the organs and systems of humans through bioaccumulation and biomagnification throughout trophic webs, leading to diseases and death (Singh et al. 2011). The sublethal toxicity and basic toxic mechanisms of Cd in crustaceans have been well investigated (Cresswell et al. 2017; Cheng et al. 2018; Zhang et al. 2019). The solubility of Cd in water is low, and it often combines with Cl^{-}, SO_4^{2-}, and other organic ligands or citrate, oxalate and other inorganic ligands to form complexes (Kubier et al. 2019). There are two main ways for Cd to invade mammalian cells: passive diffusion in the form of neutral charge complexes or through specific cell membrane channels in the form of Cd^{2+} (Thévenod 2010). Cadmium destroys biomacromolecules, such as carbohydrates, lipids, DNA and proteins, through oxidative stress. Divalent cadmium can also replace divalent essential metal ions like Ca^{2+} to combine with active centres of different enzymes and result in conformational changes, which induce activity reduction and even functional loss of these enzymes (Cuypers et al. 2010).

In recent years, studies on environmental toxicology have shown great interest in detoxification mechanisms of HM in aquatic animals (Aouini et al. 2018; Drąg-Kozak et al. 2019; Duarte et al. 2019). There are three possible detoxification mechanisms of Cd in crustaceans. Physiologically, organisms regulate the absorption rate in the short term by reducing the absorption rate and increasing the excretion rate of Cd by tissue-specific accumulation and redistribution (Rainbow 2007). Through metal particles and metal binding proteins, such as metallothionein-like proteins and heat shock proteins, organisms separate and store Cd in cells and make it unavailable for longer periods of time (Chiodi Boudet et al. 2019). In addition, organisms can prevent the oxidative toxicity of Cd through antioxidant defence (Zhang et al. 2019).

Biomarkers refer to a series of abnormal indices for different levels of biological integration at the molecular, cellular, physiological, individual, and population levels under stress (Lee et al. 2015). Biomarkers are used to identify stress sources and to predict alternations at the tissue and cellular levels, which is an early warning signal of the biological effects of environmental pollutants (Viarengo et al. 2000).

Histopathology and histochemistry are cost-effective tools to evaluate the impact of environmental pollution and toxicants on invertebrates and vertebrates, and have been widely used as biomarkers for the assessment of natural and aquacultural environments (Nunes et al. 2014). As traditional and effective research methods, these tools have many advantages. Compared with biochemical parameters, histological characteristics directly reflect the health status and comprehensive responses of organisms under specific physiological, nutritional, and environmental conditions (Vogt 1987). Next, as a result of biochemical mechanics, they integrate the damage of individuals at the molecular level (Hinton and Lauren 1990).

Accumulation of high Cd^{2+} level can induce excessive reactive oxygen species (ROS), e.g., H_2O_2, O_2^{-} and ·OH, which would break the redox balance of organisms and trigger oxidative stress (Bartosz 2009). Aerobic organisms resist oxidative stress mainly by avoiding ROS production, scavenging oxidation-reduction intermediates, preventing the initiation or extension of the respiratory chain and damage repair (Cuypers et al. 2010). The antioxidant defence system is the main mechanism to quench the surge of ROS. Superoxide dismutase (SOD) and catalase (CAT) generally form the first line of antioxidative defence (Otto and Moon 1996). Glutathione reductase (GR) and thioredoxin reductase (TrxR), as members of the sulfhydryl-dependent antioxidant system, play an important role in the phase II metabolism of xenobiotics. They participate in the oxidation-reduction cycle of glutathione (GSH) and thioredoxin (Trx), respectively, which act as a natural buffer and barrier to maintain the redox balance of the intracellular environment (Ouyang et al. 2018).

Acetylcholinesterase (AChE) terminates the nerve impulse between nerves and muscles by hydrolysing the neurotransmitter acetylcholine (ACh) (Branca et al. 2018). In addition, AChE promotes the development, maturation, and regeneration of nerve cells. When AChE level is abnormal, imbalance of Ach metabolism occurs and directly inhibits behaviour in crustaceans, such as dysfunction of swimming (Ren et al. 2015) and predation (Harayashiki et al. 2016). Therefore, AChE is an important neurotoxicity biomarker. Malondialdehyde (MDA), as a stable and abundant end product of lipid peroxidation (LPO) caused by oxidative stress, is a widely used biomarker of LPO, leading to several diseases and is valuable in their diagnosis (Niki 2009).

Crabs (Crustacea, Decapoda) are active and omnivorous with low metabolic rates. They positively connect the material exchange and energy transfer between aquatic and terrestrial animals, and are intermediaries between producers and secondary consumers within the aquatic food web. Crabs are easily affected by pollutants at multiple levels and have a certain tolerance to pollutants (Arockia Vasanthi et al. 2014). Meanwhile, they can be easily collected and acclimated. Hence, crabs are excellent indicators of environmental health (Negro and Collins 2017). Crabs are generally used in

monitoring and assessment of aquatic environmental quality and ecotoxicology research (Wiech et al. 2018; Duarte et al. 2019; Salvat-Leal et al. 2020). However, there are few reports on the mechanism of Cd elimination in crabs. In view of this, we used a representative species of crustaceans, the freshwater crab *S. henanense* to study histopathological damage, Cd bioaccumulation, and biochemical biomarkers (SOD, CAT, GR, TrxR, AChE activities and MDAcontent) of the gills and hepatopancreas, as well as macromolecular changes of the hepatopancreas, during Cd exposure and elimination. We systematically elucidate the detoxification and recovery mechanisms of crustaceans from the perspectives of micromorphology, Cd accumulation, oxidative damage, antioxidant defence, and neurotoxicity to lay a foundation for further studies of the tolerance and regulation mechanisms to HM and to use crustaceans more effectively in monitoring the quality of aquatic environments.

Materials and methods

Animal acclimation

Individuals of the freshwater crab *S. henanense* were obtained from the Wulongkou Aquatic Product Market in Taiyuan, Shanxi, China. Crabs were rinsed and kept individually in compartments for over two weeks under laboratory conditions. According to their living environment, the experimental condition was set as follows: circulating dechlorinated water at a temperature of 16.54 ± 0.41°C, dissolved oxygen of 8.52 ± 0.56 mg L^{-1}, conductivity of 5.27 ± 0.57 μS cm^{-1}, pH of 7.26 ± 0.22, and ammonia nitrogen≤ 0.05 mg L^{-1}, with a 14 h:10 h light-dark cycle. During the maintenance phase, the water volume of each culture cube was approximate 192 cm^3, and crabs were not submerged under water to ensure breathe smoothly. Crabs were feed with artificial diet (crude protein: 39.26%, crude lipid: 9.75%, provided by Shanghai Ocean University) at a ratio of 1% of their weight every two days from the second week of acclimation. After 3 h of feeding, any food left was removed using a siphon tube.

Exposure and elimination experiment

The overall design and animal treatment of the experiment are shown in Fig. S1. After acclimation, healthy and similarly sized (20.02 ± 4.15 g wet weight, 3.91 ± 0.35 cm carapace width) carbs were randomly divided into four groups of 20 crabs each, exposed to 0 (control group, CG), 50 (Treament Group 1, TG1), 100 (TG2) or 500 (TG3) μg· L^{-1} $CdCl_2$. The concentrations of Cd were selected on the basis of class III of Environmental Quality Standards for Surface Water of China (GB3838-2002) (10 times, 20 times, and 100 times 0.005 mg· L^{-1} Cd). The experiment consisted of two stages, including a Cd exposure phase lasting 14 d and a Cd elimination period for 21 d. Each group was individually placed in glass quartz aquaria (50 cm × 30 cm × 25 cm) with 2 L water. The water was changed, and feed was supplied every 48 h, when all parameters were kept the same as in the acclimation period. Experiments were performed in triplicate. The average mortality rate of each replicate was less than 5%.

The four crabs from each group were sacrificed after anaesthesia on ice for 15 min, and the small pieces of the gills and hepatopancreas (Fig. S2) were dissected rapidly on the 14th, 21st, 28th, and 35th d of the experiment.

The overall body and hepatopancreas weight of each crab was recorded for the hepatosomatic index (HSI), which is expressed in grams per 100 g body weight and calculated by the following formula:

HSI = hepatopancreas weight/body weight × 100.

Histopathological and histochemical techniques

The tissues of the gills and hepatopancreas were carefully excised, immediately fixed, and embedded in paraffin. Afterwards, sections of 4 μm thickness were cut with a rotary microtome (Leica RM 2255, Frankfurt, Germany) and stained with routine Cole's haematoxylin and eosin (H.E.). Digital images were made using a light microscope (Olympus BX51, Tokyo, Japan) with Image-Pro plus 6.0 software (Media Cybernetics, Maryland, USA). The images were examined for semi-quantitative and histopathological diagnosis as proposed by de Melo et al. (2019) with some modifications. Blind-coded labels were used to ensure objective and reasonable operation to statistics. The importance weight (w) and score (a) (Bernet et al. 1999) of histopathological evaluation in the gills and hepatopancreas were shown in Table S1. The histopathological indices (I_{his}) were calculated by Formula S1. The methods of histology and histochemistry tests were shown in Table S2. The histochemical estimation proposed by Nunes et al. (2014) was used for the analysis of the Alcian Blue and Periodic Acid Schiff (AB-PAS), Oil Red O (ORO), Feulgen, and Mercuric Bromophenol Blue (MBB) of the hepatopancreas.

Determination of Cd concentrations

The specimens were weighed and digested with 5mL HNO_3 for 2h and transferred to a high-throughput microwave instrument (Master 40, Shanghai, China) for digestion. When acid was eliminated, the samples were diluted to 10 mL with 1% HNO_3. The five-point sampling method was used to collect 2.5 mL water in the exposure stage (before water changes at 48 h). The processing method of water was as described above. The concentrations of Cd were measured with an atomic absorption spectrophotometer (Varian AA240, California, USA) at 228.8 nm according to the method described by the

Chinese National Standard for determination of Cd in food (GB 5009.15-2014). The detection limit of standard Cd solution (national standard sample, GNM-M155040-2013, China) was 0.005 μg· g^{-1}. Standard Cd solution has been withdrawn in December 2020. The carrier gas was acetylene. The bioconcentration factor (BCF) and elimination coefficient (EC), proposed by Jing et al. (2019), with some modifications, were calculated by Formulas S1 and S3.

Measurements of biochemical parameters

The gills and hepatopancreas samples were added to a cold 0.85% NaCl solution in two specifications: a ratio of 1:9 (w/v) for SOD, CAT, AChE, MDA, and a ratio of 1:4 (w/v) for GR and TrxR. The samples were homogenized by an automatic homogenizer (JXFSTPRP-11, Shanghai, China) and centrifuged at 8000 rpm for 10 min at 4°C. The supernatant was used to measure biochemical parameters following the manufacturer's protocol described by the kits (Solarbio Science and Technology Co., Ltd., Beijing, China). All measurements (triplicate) were performed with a microplate reader (Spectra max M5, Molecular Devices, California, USA).

SOD activity was measured according to Nishikimi (1975) and calculated by measuring the rate of absorbance decline at 560 nm. The CAT activity was determined according to the decreasing rate of absorbance at 240 nm (Johansson and Borg 1988). The GR activity was detected according to the decreasing rate of absorbance at 340 nm (Mannervik 2001). The TrxR activity was measured based on the increasing rate of absorbance at 412 nm (Arnér et al. 1999). The AChE activity was determined according to the increase in rate of absorbance at 412 nm (Ellman et al. 1961). MDA content was determined by a method based on reaction with thiobarbituric acid at 532 nm and 95°C (Ohkawa et al. 1979). Protein content was determined according to Bradford (1976) using bovine serum albumin as a standard.

Principal component analysis

Principal component analysis (PCA) was employed to summarize the data of each treatment group with different histopathological and biochemical alterations in this work. Our data were projected onto the first few principal components (PCs), with eigenvalues> 1.0 (Kaiser's rule), to identify the pattern and cluster of the specimens depending on their variance. We retained the factor loading of variables between -1 and 1. Generally, PC1 is defined as a direction that maximizes the variance of the projected data. The higher accumulation of explain variable in PC, the greater contribution to the analysis of original data. The variables far from the origin are fully explained, and adjacent variables show associations. The confidence intervals represented by ellipses are 95%.

Statistical analysis

The data were calculated and analysed using SPSS Statistics 26.0 software (IBM, New York, USA). Data distribution and the homogeneity of variance were tested using Shapiro-Wilk test and Levene's test. Significant intergroup differences were determined by one-way ANOVA and Tukey's post hoc test after meeting the prerequisites. The correlation matrix was calculated to show the relationships among Cd content, histopathological alternations and biochemical parameters. The results are presented as mean ± S.D. (n=4) and were obtained using GraphPad Prism 8.0 software (GraphPad Software, California, USA) and R software version 2.15 (Tsinghua University, Beijing, China).

Results

HSI change records

The changes in HSI of *S. henanense* were shown in Table 1. After Cd exposure, the HSI of all treatment groups were significantly decreased (p< 0.05). After 7 and 14 d of depuration, only the HSI of TG3 (500 μg· L^{-1} Cd group) was significantly lower than CG (control group).

Cd bioaccumulation and elimination

After exposure, the Cd level in the gills and hepatopancreas showed a significant increase (p< 0.05) in a dose-dependent manner (Fig. 1 a, b). The maximum Cd content was 14.53 ± 1.73 μg· g^{-1} ww found in the gills of TG3. The Cd content of crabs returned to baseline at 35th d, except for TG3. The BCF of the gills of TG1 (50 μg· L^{-1} Cd group) and TG2 (100 μg· L^{-1} Cd group) was significantly higher than that of the hepatopancreas (Fig. 1 c), and the EC of the gills of TG2 and TG3 was significantly larger (Fig. 1 d). The gills of TG1 had maximum BCF (9.51 ± 2.85%) and EC (65.11 ± 9.80%).

Histopathological observations and examinations

Normal and healthy gills of *S. henanense* were composed of a central branchial stem with dense and regular lamellae on the sides (Fig. 2 a1). Both the branchial stem and lamellae consisted of thin cuticle and monolayer epithelial cells that were closely connected to the cuticle. The branchial stem contained nephrocytes, also known as podocytes, which were rich in vacuoles. Pillar cells and a few haemocytes in the lamellae were characteristic and regularly distributed. The epithelial cells joined the nucleus to form haemolymph vessels at certain intervals in the lamellae. The interlamellar spaces were 18.06 ± 2.57 μm, with a water channel aligned parallel to one another. The periphery of each lamella expanded to form a marginal channel.

Table 1 HSI of the control and treated *S. henanense* after 14 d of exposure and 21 d of depuration

Groups	HSI in 14th d	HSI in 21st d	HSI in 28th d	HSI in 35th d
CG	3.76 ± 0.13 ^{ef}	3.94 ± 0.21 ^{f}	4.04 ± 0.15 ^{f}	3.70 ± 0.22 ^{ef}
TG1	3.06 ± 0.41 ^{bcd}	3.68 ± 0.09 ^{ef}	3.89 ± 0.36 ^{f}	3.60 ± 0.11 ^{def}
TG2	2.75 ± 0.28 ^{ab}	3.49 ± 0.34 ^{cdef}	3.55 ± 0.20 ^{def}	3.55 ± 0.18 ^{def}
TG3	2.34 ± 0.18 ^{a}	2.71 ± 0.22 ^{ab}	2.90 ± 0.13 ^{abc}	3.29 ± 0.27 ^{bcde}

Significant differences ($p< 0.05$, Tukey's post hoc test) were indicated by different letters between groups, n=4. CG: Control; TG1: 50 μg· L^{-1} Cd; TG2: 100 μg· L^{-1} Cd; TG3: 500 μg· L^{-1} Cd

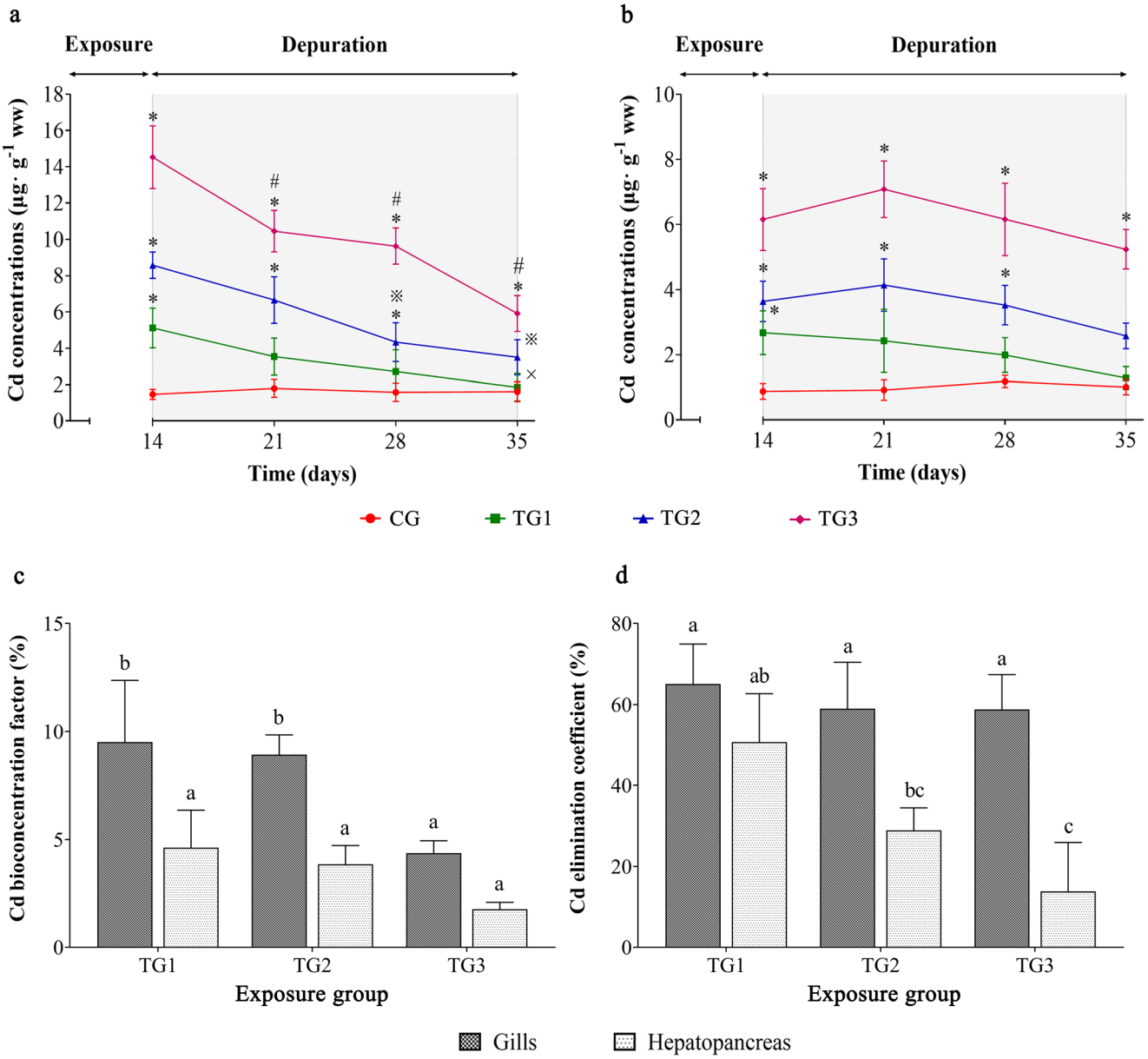

Fig. 1 Cd concentrations (**a**: gills, **b**: hepatopancreas), bioconcentration factor (**c**) and elimination coefficient (**d**) of *S. henanense* after exposure and depuration. Comparison between the treatment and control groups at the same time point: $^{*}p< 0.05$; Comparison of treatment groups before and after depuration : $^{\times}p< 0.05$ (TG1), $p< 0.05$ (TG2), $^{\#}p< 0.05$ (TG3). There was a significant difference among the groups represented by different letters ($p< 0.05$). CG: Control; TG1: 50μg· L^{-1} Cd; TG2: 100μg· L^{-1} Cd; TG3: 500μg· L^{-1} Cd. Mean ± SD, n=4

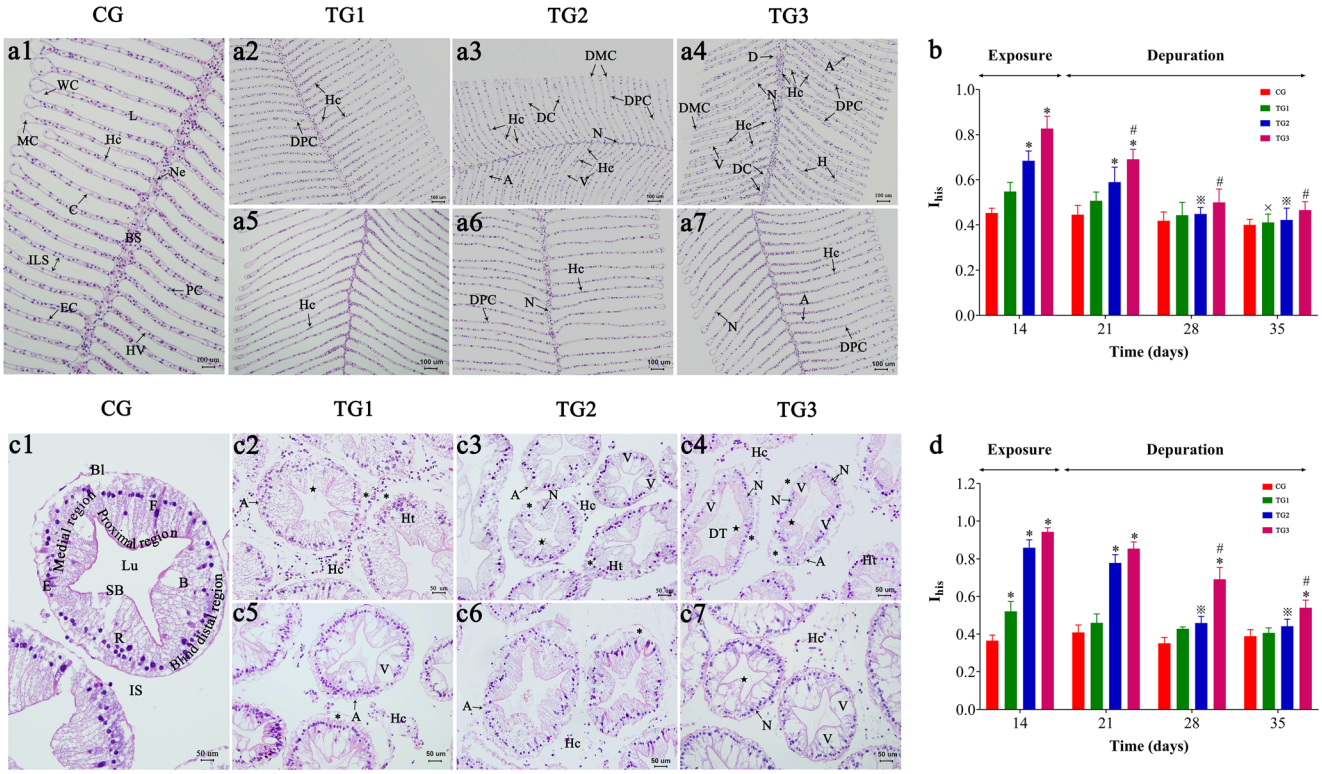

Fig. 2 The light micrographs stained with H.E. (**a1-a7**: gills, **c1-c7**: hepatopancreas) and I_{his} (**b:** gills, **d:** hepatopancreas) of *S. henanense*. (**a1**) Control group exhibited normal gills structure: branchial stem (BS) contained nephrocytes (Ne), lamellae (L) contained pillar cells (PC) and a few haemocytes (Hc), cuticle (C) with a thin layer of epithelial cells (EC), sound marginal canal (MC), equal interlamellar spaces (ILS), full haemolymph vessels (HV) and clean water channels (WC). (**a2-a4**) The gills of TG1, TG2 and TG3 showed the lesions of destroyed pillar cells (DPC), hyperplasia (H), disrupted cuticle (DC), necrosis (N), vacuolation (V), deposits (D), atrophied lamellae (A) and damaged marginal canal (DMC). (**a5-a7**) The TG1 recovered after 7 d of depuration, and TG2 and TG3 repaired after 14 d of elimination. Bars = 100 μm. (**c1**) The normal structure of the hepatopancreas: star-like lumen (Lu), tight intertubular space (IS), intact striated border (SB) and basal lamina (Bl). The epithelium consists of embryonic cells (E), resorptive cells (R), fibrillar cells (F) and blister-like cells (B). (**c2-c4**) The hepatopancreas of TG1, TG2 and TG3 indicated mild to severe damage, such as hypertrophy (Ht), disrupted membrane (★), atrophy (A), necrosis (N), disrupted tubules (DT), vacuolation (V), increased haemocyte (Hc) and epithelial detachment (*). (**c5-c6**) The destroyed structure of the hepatopancreas from TG1 and TG2 restored at 21st and 28th d, respectively. (**c7**) The lesions exposed to 500 μg· L^{-1} Cd did not disappear completely even at the end of clearance. Bars = 50 μm. Comparison between the treatment and respective control groups: $^{*}p< 0.05$; Comparison of treatment groups before and after depuration : $^{\times}p< 0.05$ (TG1), $p< 0.05$ (TG2), $^{\#}p< 0.05$ (TG3). CG: Control; TG1: 50 μg· L^{-1} Cd; TG2: 100 μg· L^{-1} Cd; TG3: 500 μg· L^{-1} Cd. Mean ± S.D., $n = 4$

In contrast, after Cd exposure, the number of haemocytes were slightly increased, and pillar cells were degraded in the lamellae, which were deformed mildly in TG1 (Fig. 2 a2). Further injuries were observed in TG2. The arrangement of lamellae was completely disorganized, and marginal canals varied in size. Damaged pillar cells, atrophied lamellae, disrupted cuticles, vacuolation and necrosis in epithelial cells were observed. The number of haemocytes increased. The interlamellar spaces were unequal and disordered (Fig. 2 a3). The injuries in TG3 were the most severe. The lamellae showed epithelial hyperplasia, wavy bulge and breakage because of the small number of pillar cells. Haemocytes were sharply in number and clogged the haemolymph vessels. Furthermore, in TG3, some nephrocytes disappeared, and deposits and vacuoles in epithelial cells were present casually. The water channels were affected by further damaged marginal canals (Fig. 2 a4). An increase in the number of haemocytes was observed in TG1 after 7 d of depuration (Fig. 2 a5). The numbers of necrotic epithelial cells, destroyed pillar cells and haemocytes were declined, and atrophy was alleviated in TG2 and TG3 after 14 d of elimination (Fig. 2 a6, a7). Histopathological data showed that the damage in TG2 and TG3 was significant ($p< 0.05$) after exposure, and their I_{his} decreased to the control level after 14 d of clearance where they were maintained until the end of the experiment (Fig. 2 b).

As shown in Fig. 2 c1, the hepatopancreas of healthy *S. henanense* was composed of several densely packed branching tubules that were composed of a single layer of high columnar or conical epithelial cells and basal lamina coated with epithelium. Each hepatic tubule was differentiated into three regions: blind distal, medial, and proximal. The blind distal and medial regions constitute the lumen, which forms the cortical region of the hepatopancreas while the proximal

region forms the medullar region. The lumens were star or cross shaped, with a diameter of 505.46 ± 132.71 μm in cross section. The inclusions of the lumen, the complete striated border and the microvilli attached to them were clearly visable. The hepatopancreatic epithelium had four cellular types: embryonic cells (E-cells), resorptive cells (R-cells), fibrillar cells (F-cells) and blister-like cells (B-cells). The F-, R-, and B-cells were mainly distributed in the proximal and medial parts of the hepatic tubules. Among them, the number of R-cells was highest. F-cells were commonly located between R- and B-cells. The E-cells, the least in number, were mainly distributed in the blind distal region.

After 14 d Cd exposure, atrophy of the epithelium of the hepatic tubules in TG1 was observed, with some epithelial cells dislodged from the basal lamina. Disrupted membranes, infiltrated haemocytes and hypertrophied cells were also observed (Fig. 2 c2). The hepatic tubules were deformed, and epithelial cells were fuzzy and oedematous in TG2. The vacuolation and necrosis of epithelial cells appeared occasionally at 14th d (Fig. 2 c3). Upon 500 μg·L-1 Cd exposure, the hepatic tubules became disordered and degenerated, and vacuolation and necrosis of epithelial cells boosted. It was difficult to distinguish the types of epithelial cells. Moreover, increased numbers of F-and B-cells in the hepatopancreas were observed as well as reduction in R-cells at 14th d (Fig. 2 c4). The injuries of disruption, haemolytic infiltration and hypertrophy vanished, and vacuolation emerged in TG1 after 7 d of depuration (Fig. 2 c5). Only detached and atrophied epithelium was observed occasionally in TG2 at 28th d (Fig. 2 c6). Mild vacuolation and necrosis in epithelial cells were still observed, but the basal lamina was relatively intact and closely connected to the epithelium in TG3 at the end of depuration (Fig. 2 c7). The Ihis of hepatopancreas was significantly increased, and in a concentration-dependent manner under Cd exposure. The Ihis in TG1 and TG2 were returned to the baseline level at 21st and 28th d. Yet in TG3, Ihis was still significantly higher than the control level after 21 d of purification (Fig. 2 d). All histopathological images during the experimental period were provided in Online Resource 1 and 2.

Histochemical observations and evaluations

After stained with AB-PAS, abundant neutral and acid polysaccharides were found in the vacuoles of B-cells and R-cells in the hepatic tubules of control crabs, respectively. The plasma membrane of epithelial cells, especially in the striated border, and haemolymph and lumen also showed a few polysaccharides. Additionally, we observed in the control group that the F-cells showed a weak positive reaction, while E-cells showed negative (Fig. 3 a1). Upon 500 μg· L^{-1} Cd exposure, the B-cells vacuoles showed a weak positive reaction with almost no neutral polysaccharides, and the cytomembrane indicated a strong positive reaction with increasing neutral polysaccharides (Fig. 3 a2). After 21 d of depuration, the impact of Cd on carbohydrates in the hepatopancreas was offset and re-accumulation of neutral polysaccharides in vacuoles was observed (Fig. 3 a3).

The neutral lipids stored in the cytoplasm of normal hepatopancreatic cells were shown by the ORO reaction, which exhibited a bright-red colour, complete and plump neutral lipids. Moderate positive reactions were also observed around the nucleus (Fig. 3 b1). After exposure, the size and density of neutral lipids decreased, and their distribution was scattered in TG3 (Fig. 3 b2). The neutral lipids were restored, and their size, density, and distribution were the same to the control group, as well as their shape, at the end of the experiment (Fig. 3 b3).

The nuclei of the four epithelial cells in the hepatopancreas were purple and round- or oval-shaped in the control crabs as shown using the Feulgen reaction. The nuclei were not uniform in size, and most of them were located at the base of cells. The nuclear envelope, the evenly distributed fine chromatin and the intermediate or deviated nucleolus became clearly visible (Fig. 3 c1). Agglutinated chromatin, unclear boundary of the nucleus and nucleolus, and apoptosis and necrosis appeared in the cells of crabs exposed to 500 μg· L^{-1} Cd (Fig. 3 c2). After 21 Cd elimination, the injuries to the nucleus were alleviated, while apoptosis and necrosis were still observed in TG3 (Fig. 3 c3).

The total proteins were stained blue by the MBB reaction in CG, protein granules were found evenly distributed in the cytoplasm and around the nucleus of the epithelial cells, and they were also observed in the vacuoles of R-and B-cells. Moreover, F-cells were positive, but E-cells were negative (Fig. 3 d1). After exposure, a strong reaction of the striated border and lightly decreased protein granules were observed in TG3 (Fig. 3 d2). The protein particles were restored at the end of the experiment (Fig. 3 d3). All histochemical pictures of macromolecules from 14^{th} to 35^{th} d were provided in Online Resource 3-6.

As shown in Table 2, the AB-PAS and ORO reaction intensity weakened but the Feulgen reaction intensity strengthened after Cd exposure. DNA damage was repaired rapidly during 14 d of depuration, and the destruction of polysaccharides and neutral lipids was also restored before the end of the depuration. The total proteins were always strongly positive regardless of exposure or clearance.

Alternations in biochemical biomarkers

In the treatment groups, SOD activity was significantly inhibited in the gills ($p< 0.05$) but was significantly activated in the hepatopancreas after Cd exposure, except in TG3. SOD activity in all treatment groups returned to control level at 28^{th} and 35^{th} d (Fig. 4, a1, a2). CAT activity in the hepatopancreas was significantly activated in crabs exposed to Cd, and the

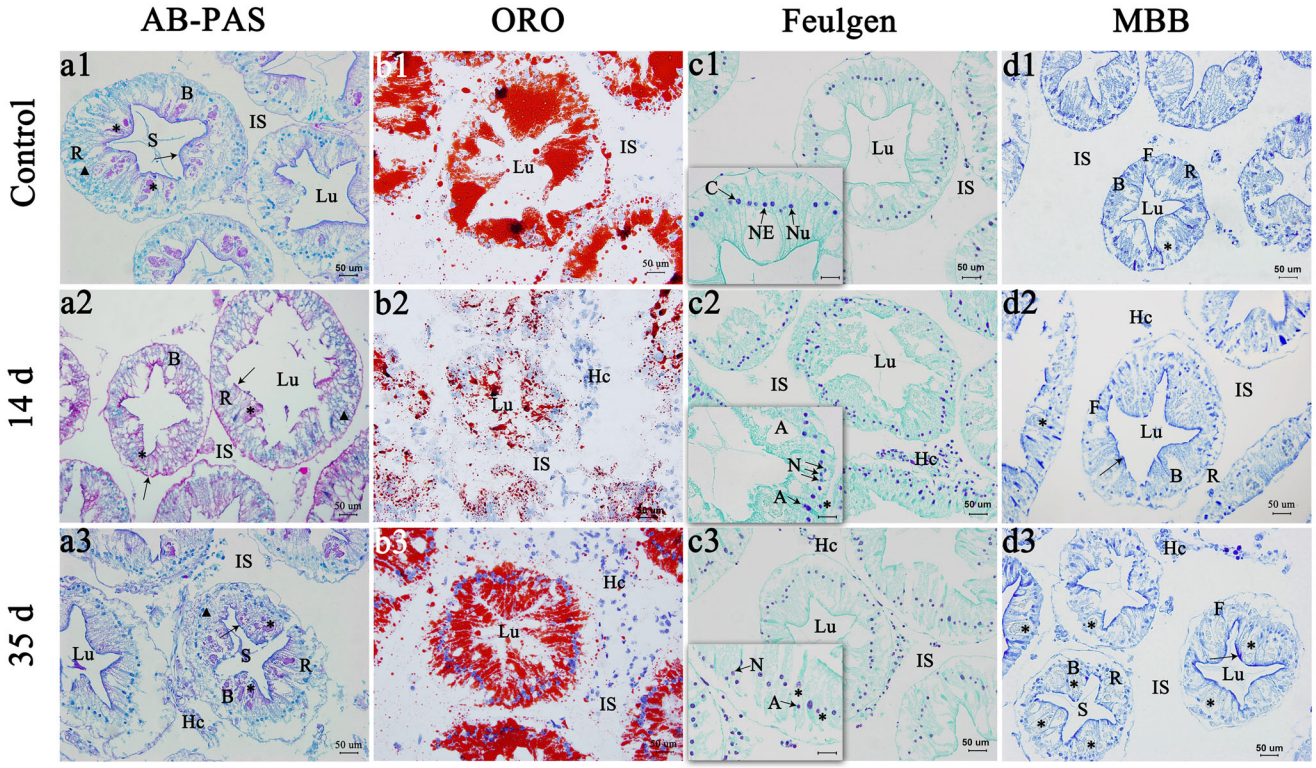

Fig. 3 The sections of the hepatopancreas of *S. henanense* exposed to 500 μg· L^{-1} Cd by AB-PAS, ORO, Feulgen and MBB histochemical tests. (**a1**) Control revealed abundant neutral polysaccharides (*) and acid polysaccharides (▲), mainly in blister-like cells (B) and resorptive cells (R), respectively. A few polysaccharides in the lumen (Lu), plasma membrane (↑) and intertubular space (IS). (**a2**) The evident reduction of neutral polysaccharides in B-cells and a rise of neutral polysaccharides in the cytomembrane. (**a3**) The storage of carbohydrates raised. (**b1**) The strongly positive reaction and rich neutral lipids (red colour) in the healthy crabs. (**b2**) Stored lipid content were decreased. (**b3**) Neutral lipids accumulated again. (**c1**) Control individuals showed normal morphology of epithelial cell nuclei, including complete nuclear envelope (NE) and nucleolus (Nu), as well as evenly distributed chromatin (C). (**c2**) The agglutinated chromatin, unclear boundary of nucleus and nucleolus (*), and apoptosis (A) and necrosis (N) of epithelial cells in the treatment group. (**c3**) Most of the damaged nuclei of epithelial cells recovered. (**d1**) The rich total proteins of hepatic tubules and protein granules (*) in vacuoles of B-cells and R-cells. (**d2**) The increased secretion of proteins in the cytomembrane (↑) (**d3**) Strongly positive reaction in epithelial cells of hepatopancreas. Lu: lumen; IS: intertubular space; Hc: haemocyte; S: secretion. Bars = 50 μm; Small images (10×60)

activity in both the gills and hepatopancreas after depuration were the same as control crabs (Fig. 4 b1, b2). The significantly elevated GR activity of the gills and hepatopancreas was exhibited under Cd stress. GR activity of the gills recovered before the end of depuration. Yet in TG1 and TG3, GR activity of the hepatopancreas remained at a significant high level during depuration (Fig. 4 c1, c2). A significantly inhibited TrxR activity of the gills in TG3 and significantly activated TrxR activity of the hepatopancreas in TG1 and TG2 were observed after exposure. TrxR activity returned to control level at 35th d, except in TG3 (Fig. 4, d1, d2). AChE activity was significantly activated after exposure, other than in the hepatopancreas of crabs exposed to the 500 μg· L^{-1} Cd. Restoration of AChE activity appeared after 7 d of depuration (Fig. 4, e1,

Table 2 Histochemical reactions of the hepatopancreas of *S. henanense* during 14 d of exposure and 21 d of depuration

	CG				TG1				TG2				TG3			
	14 d	21 d	28 d	35 d	14 d	21 d	28 d	35 d	14 d	21 d	28 d	35 d	14 d	21 d	28 d	35 d
AB-PAS	++++	++++	++++	+++	+++	++	+++	++++	++	++	+++	++++	+++	++	+++	++++
ORO	++++	++++	++++	++++	+++	++++	++++	++++	++	++	++++	++++	+	++	+++	++++
Feulgen	+	+	+	+	+	+	+	+	++	+	+	+	++	++	+	+
MBB	++++	++++	++++	++++	+++	++++	++++	++++	+++	++++	++++	++++	+++	+++	++++	++++

+: weak reaction; ++: moderate reaction; +++/++++: strong reaction; CG: Control; TG1: 50 μg· L^{-1} Cd; TG2: 100 μg· L^{-1} Cd; TG3: 500 μg· L^{-1} Cd

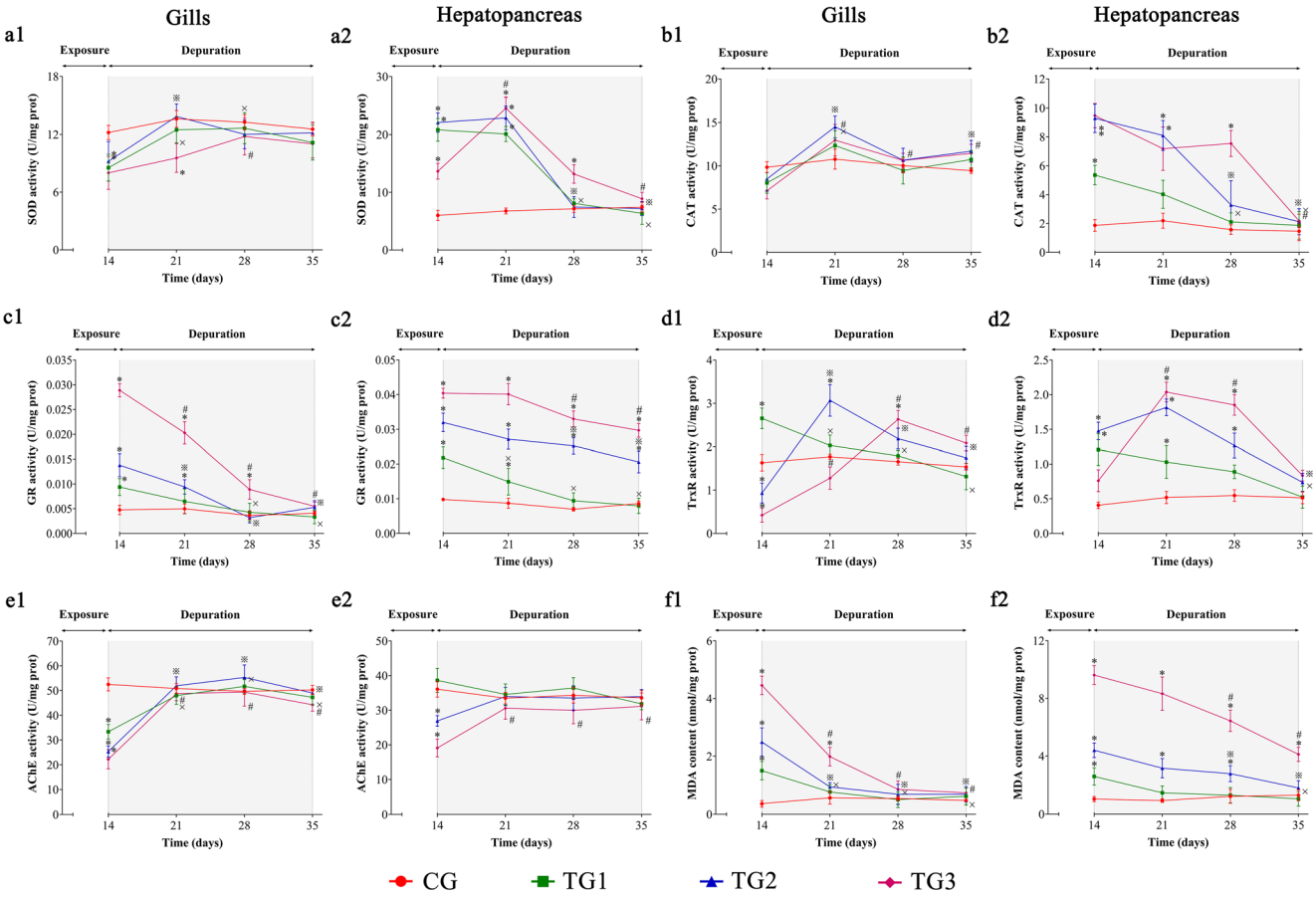

Fig. 4 The SOD, CAT, GR, TrxR, AChE activities and MDA content in the gills (a1-f1) and hepatopancreas (a2-f2) of *S. henanense* upon exposure and depuration. Comparison between the treatment and control groups at the same time point: $^{*}p< 0.05$; Comparison of treatment groups before and after depuration : $^{\times}p< 0.05$ (TG1), $p< 0.05$ (TG2), $^{\#}p< 0.05$ (TG3). CG: Control; TG1: 50 μg· L^{-1} Cd; TG2: 100 μg· L^{-1} Cd; TG3: 500 μg· L^{-1} Cd. Mean ± S.D., n=4

e2). The MDA content in all treatment groups significantly increased upon Cd exposure and it descended to the control level at 28th and 35th d in the gills of all treatment groups and also in the hepatopancreas of TG1 and TG3 (Fig. 4, f1, f2).

Correlation analysis

As shown in Table 3, in *S. henanense*, a positive correlation ($p< 0.05$) was found between Cd concentration and the following biomarkers: I_{his}, CAT, GR and MDA, and Cd concentration was negatively correlated with HSI and AChE. I_{his} showed association with several biomarkers such as CAT and GR in both the gills and hepatopancreas. Tissue-specific associations among the biomarkers were also found. For example, TrxR was only associated with other antioxidant markers in the hepatopancreas. Similarly, AChE was only positively correlated with SOD in the gills. Furthermore, MDA was positively correlated with I_{his} and GR in the gills, as well as CAT in the hepatopancreas. Additionally, HSI showed negative associations with I_{his}, CAT, GR and MDA.

The changes of all tested biomarkers of the gills and hepatopancreas were summarized in Table 4. After Cd exposure, cellular and biochemical biomarkers were abnormal in *S. henanense*. All of them recovered during the depuration period

Principal component analysis

We obtained a global vision by visualizing the data in the PCA biplot (Fig. 5). The quantitative variables represented by corresponding tested biomarkers established the pattern related to Cd content in *S. henanense* under different stages of the experiment. In Fig. 5 a, the first two factorial axes were retained that explained 78.52% of the total variance. Factor 1 (Eigen value of 5.07) displayed 63.4%, and factor 2 (Eigen value of 1.21) explained 15.12% of the total variance. In the hepatopancreas, 85.29% of the total variance was explained, where PC1 (Eigen value of 5.74) and PC2 (Eigen value of 1.17) explained 71.68% and 13.61% of the total variance, respectively (Fig. 5 b). The analysis of ellipses completed by the squared cosines and correlation map to characterize the

Table 3 The correlation coefficient among the Cd content and tested biomarker in *S.henanense* after Cd exposure

		Cd	HSI	I_{his}	SOD	CAT	GR	TrxR	AChE
Gills	I_{his} (SW:0.375)	0.945*							
		P							
	SOD (SW: 0.881)	−0.636		−0.538					
		P		P					
	CAT (SW: 0.538)	−0.674		−0.670*	0.269				
		P		P	P				
	GR (SW: 0.013)	0.951*		0.918*	−0.676	−0.556			
		S		S	S	S			
	TrxR (SW: 0.253)	−0.609		−0.543	0.106	0.303	−0.647		
		P		P	P	P	S		
	AChE (SW: 0.029)	−0.900*		−0.865	0.571*	0.683	−0.903	0.594	
		S		S	S	S	S	S	
	MDA (SW: 0.104)	0.953*		0.954*	−0.633	−0.493	0.953*	−0.690	−0.876*
		P		P	P	P	S	P	S
Hepatopancreas	HSI (SW:0.183)	−0.874*							
		P							
	I_{his} (SW:0.013)	0.924*	−0.905*						
		S	S						
	SOD (SW: 0.033)	0.682	−0.368	0.338					
		S	S	S					
	CAT (SW: 0.039)	0.788*	−0.715*	0.809*	0.526				
		S	S	S	S				
	GR (SW: 0.098)	0.913*	−0.843*	0.959*	0.344	0.847*			
		P	P	S	S	S			
	TrxR (SW: 0.108)	0.219	−0.392	0.326	0.909*	0.603*	0.407		
		P	P	S	S	S	P		
	AChE (SW: 0.377)	−0.825*	0.686	-0.618	0.068	−0.700	−0.612	−0.025	
		P	P	S	S	S	P	P	
	MDA (SW: 0.015)	0.924*	−0.835*	0.938*	0.341	0.874*	0.959*	0.374	−0.771*
		S	S	S	S	S	S	S	S

SW Shapiro-Wilks's test, *S* Spearman's correlation coefficient, *P* Pearson's correlation coefficient, * $p < 0.05$

loading factors. In the two biplots, control ellipse was projected in the negative sides of the first factorial axes. The gills of TG1 was projected in the negative sides of the two factorial axes, and the 50 μg· L^{-1} Cd treated hepatopancreas were projected in the negative sides of the first and positive sides of second factorial axes. The gills and hepatopancreas exposed to 100 μg· L^{-1} Cd were projected around the origin and both in the positive and negative sides of the two factorial axes. The gills of TG3 was projected in the positive sides of the two factorial axes, and the counterpart of TG3 were

Table 4 Summary of biomarkers changes detected in *S. henanense*

	Cd content	HSI	I_{his}	Biomacromolecules	SOD	CAT	GR	TrxR	AChE	MDA
Exposure (0–14thd)	↑ (G, H); G> H	↓	↑ (G, H)	↓ (P, L) ↑ (DNA)	↓ (G) ↑ (H)	↑ (H)	↑ (G, H)	↓ (G) ↑ (H)	↓ (G, H)	↑ (G, H)
Depuration (14th–35thd)	R (G★, H)	R	R (G★, H)	R (P, L, DNA★)	R (G★, H)	R (G★, H)	R (G)	R (G, H)	R (G★, H★)	R (G★, H)

↑: increase; ↓: decrease; G: gills; H: hepatopancreas; *R*: recovery; ★: recovery fast; *P*: polysaccharides; *L*: lipids

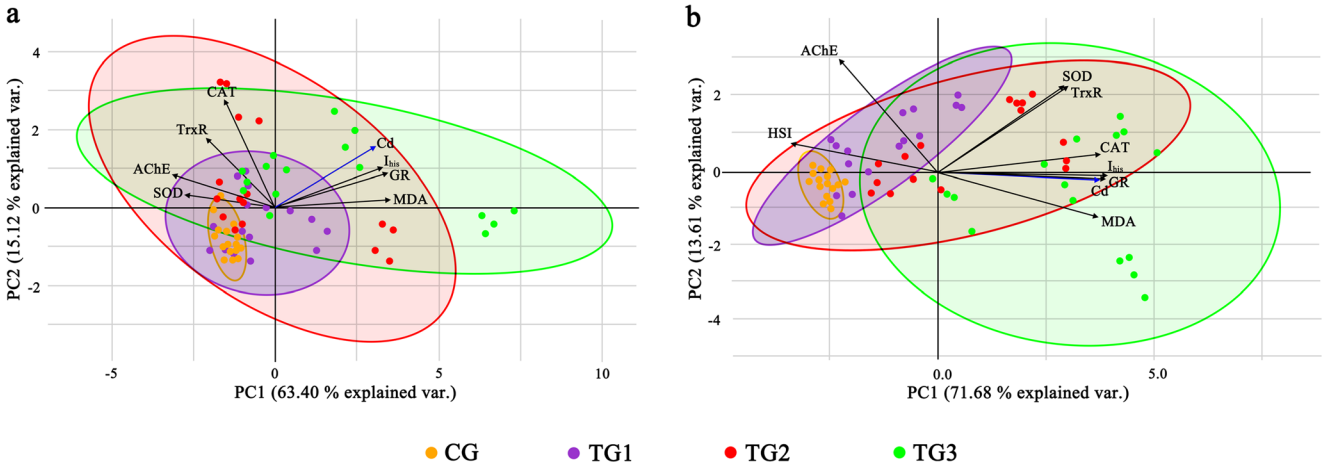

Fig. 5 PCA biplots were employed for analysis of histopathological and biochemical variables in *S. henanense* (**a** gills; **b** hepatopancreas) during the experiment. Projection of the variables and the cases on the factor-plane (1×2). CG: Control; TG1: 50 μg· L^{-1} Cd; TG2: 100 μg· L^{-1} Cd; TG3: 500 μg· L^{-1} Cd

projected in the positive sides of the first factorial axes. Moreover, in the two biplots, the individuals of TG3 had a significant difference ($p< 0.05$) compared with the control.

Discussion

Cadmium contamination in water has not been well dealt with for a long time (Singh et al. 2011; Chiodi Boudet et al. 2015; Duarte et al. 2019). Our results provide information of detoxification in the freshwater crab *S. henanense*, which promote the development of biomarkers in benthic crustaceans that are conducive to environmental monitoring.

In toxicological studies, organ index is a generally used biomarker as the apparent ratios of organs to body mass, which is associated with changes in the environment (Iheanacho and Odo 2020). The HSI, representing the relative weight of hepatopancreas, decreased significantly ($p< 0.05$) after Cd exposure (Table 1). The presented results were coincided with those published by Revathi et al. (2011) and Jamwal et al. (2018), on the impact of Cd on HSI of the prawn *Macrobrachium rosenbergii* and the fish *Oncorhynchus mykiss*. Drąg-Kozak et al. (2019) showed that the reduction in HSI was attributed to the necrotic and degenerative hepatopancreatic cells and energy depletion. Our histopathological and histochemical results (Fig. 3 a2, b2 and c2) confirmed these findings.

The characteristic of accumulation and selectivity of elimination to Cd were analysed, by determining Cd concentrations in the gills and hepatopancreas of *S. henanense*. Several studies reported that crabs reflected the bioavailability of HM in water environment due to their nature of accumulation of waterborne substances (Bordon et al. 2018; Cheng et al. 2018; Salvat-Leal et al. 2020). In this study, Cd levels in the gills and hepatopancreas remarkably elevated ($p< 0.05$) when the crabs exposed to different Cd concentrations (Fig. 1 a, b). Generally, these two organs are the target organs for HM accumulation, since environmental pollutants mainly enter crustaceans through water and food (Jerome et al. 2017). The BCF explained higher Cd accumulation of the gills in *S. henanense* (Fig. 1 c). We observed that the lamellae, which directly contacted with the water and easily retained pollutants, were dense and aplenty (Fig. 2 a1). Bordon et al. (2018) made a similar observation in the crab *Callinectes danae*, and held that the gills were vulnerable to HM because of continuous filtration. The discrepancy of Cd bioconcentrations in different organs is associated with uptake rate, organic function and polluted background (Ahearn et al. 2004). The uptake rate of HM by the gills mainly depends on waterborne dissolution rate, but the uptake rate of HM transferred into the hepatopancreas is determined by complicated multiple factors like digestion rate and assimilation efficiency (Rainbow 2007). Duarte et al. (2019) reported that the pristine crabs *Ucides cordatus* showed higher Cd concentrations in the gills whereas in impacted crabs, the Cd content in the hepatopancreas was higher due to detoxification.

Organisms need to continuously discharge toxins to resist toxicity, especially for Cd and other HM with the long half-life. The concentrations of bioavailable HM will not exceed the toxic threshold in crustaceans, so long as the combined excretion rate is higher than the uptake rate (Marsden and Rainbow 2004). The elimination effects varies with factors such as health status, water temperature, depuration time and HM concentrations (Jing et al. 2019). Cresswell et al. (2017) investigated the elimination of isotope ^{109}Cd in the prawn *Macrobrachium australiense*, and discovered that Cd content in the hepatopancreas did not decrease consecutively during depuration followed by acute exposure (0.56 μg· L^{-1} ^{109}Cd, 7d). In the present study, the Cd residual of hepatopancreas also increased slightly after 7d of elimination (Fig. 1 b),

indicating the vital role of the hepatopancreas in Cd storage and sequestration. Similar phenomenon was reported by Drąg-Kozak et al. (2019), who suggested that Cd saturation of other organs was responsible for repeated Cd accumulation of the liver in the carp *Carassius gibelio* during the depuration period. Many trace metals, including Cd, are transferred from other organs to hepatopancreas through haemolymph and further discharge into water in the form of metallothionein and metal granules (Wiech et al. 2018). Crustaceans are able to regulate HM concentrations in different organs individually to minimize the adverse effect of excessive HM, which is an effective physiological means of detoxification (Ahearn et al. 2004; Dan et al. 2019). In the present work, the EC reflected the excretion effects, and the gills showed higher elimination capacity (Fig. 1 d). The dissolved metals are rapidly removed in a concentration gradient when gills are in contact with the clean water, whereas granular metals stored in hepatopancreas need more time to be discharged (Lemus et al. 2016). Therefore, the gills are considered an excretory site besides antennal gland in crustaceans (Ahearn et al. 2004). Our data also supported several previous studies in aquatic animals on HM elimination (Li et al. 2007; Aouini et al. 2018; Jing et al. 2019), and these authors reported that gills had fastest elimination rates compared with other organs. Furthermore, the gills are the important organ that contribute to Cd elimination, and the hepatopancreas has a potential ability to manipulate integrally Cd level for metabolic profit in *S. henanense*. The subcellular distribution of HM during depuration will be investigated in our further researches to comprehend the mechansims of detoxification in crabs.

Histopathology is extensively used to comprehensively assess the impacts of stress on organisms. In our study, the histopathological injuries in the gills were easily observed upon exposure, even at low Cd concentrations, which including the lesions of missing pillar cells and nephrocytes, clogged haemolymph vessels, irregular and atrophied lamellae, fractured cuticles, hyperplasia, deposits, vacuolation and necrosis (Fig. 2 a2-a4; Online Resource 1). The sensitivity of the gills to pollutants is closely related to their structure and function. To aquatic animals, the gills are responsible for gas exchange, osmotic ion regulation, acid-base balance and other functions, as well as a primary site against pollutants invasion (Negro and Collins 2017). Similar injuries in the contaminated gills were published by Arockia Vasanthi et al. (2014) and do Carmo et al. (2018), on the crab *Scylla serrata* and the fish *Prochilodus lineatus*, respectively. The deformed and atrophied lamellae are early histopathological markers showing the adverse impacts of toxins on aquatic species (Mansouri et al. 2016). The superfluous haemocytes and deposits block haemolymph vessels, which further cause the dramatic circulatory and respiratory failure, even hypoxia and asphyxia (Jerome et al. 2017). These dysfunctions also result from the hyperplasia of the epithelium. do Carmo et al. (2018) showed that the dilatant marginal canals caused pillar cells destruction and degradation in the gills. Although the dilatation of marginal canal was not obvious, the severely damaged pillar cells were ascribed to congestion in this study. We speculate that this lesion is the relevant result of growing oxygen demand to aerobic organisms to resist dyspnea caused by swelling, increased haemocytes and hyperplasia. Certainly, this hypothesis needs further researches for verifications.

In crustaceans, the hepatopancreas, as a multi-functional organ, is capable of detoxification, nutrients absorption, synthesis of digestive enzymes and immune response, as well as gonadal development (Vogt 2019). We observed the four types of epithelial cells (E-, F-, B-, and R-cells) of the hepatopancreas (Fig. 2 c1; Online Resource 2), as described by Cheng et al. (2018) and Zhang et al. (2019). However, the hepatopancreatic epithelium consists of five types cells (E-, F-, B-, R-, and M-cells) in other crustaceans such as the shrimp *Farfantepenaeus brasiliensis* (Nunes et al. 2014) and the prawn *Macrobrachium rosenbergii* (Silva et al. 2018) because of a different cell differentiation model. The hepatopancreas is vulnerable to HM (Arockia Vasanthi et al. 2014; Chiodi Boudet et al. 2015; Bordon et al. 2018), pesticides (Negro and Collins 2017; de Melo et al. 2019; Sharma and Jindal 2020) and other toxins. In our study, a series of histopathological alternations in the hepatopancreas was found after Cd exposure, including thickened membrane, change in the number of different types of cells, increased haemocytes, vacuolation, apoptosis and necrosis. These lesions are common and typical in crustaceans, which have been previously published in the prawn *Macrobrachium rosenbergii* (Revathi et al. 2011) and the shrimp *Palaemonetes argentinus* (Chiodi Boudet et al. 2015). The haemocytes, as a basic defence, play the role of detoxification, innate immunity and cells communication. The increase in haemocyte number accelerates the transport of HM ions to the excretion site, which accomplished by a series of reactions, involving phagocytosis, nodule formation, and encapsulation (Ahearn et al. 2004). Apoptosis and necrosis, as acute phase responses, remove injured molecules and debris, and activate the repair processes (Jerome et al. 2017). Chetoui et al. (2019) reported that the haemolytic infiltration, apoptosis and necrosis were relevant to ROS production and oxidative stress. Our findings on increased F-and B-cells and decreased R-cells (Fig. 2 c3, c4) were also observed in the crab *Zilchiopsis collastinensis* after chlorpyrifos exposure (Negro and Collins 2017). These authors stated that a rise in F-and B-cells implied enhanced abilities of synthesing enzymes and excreting xenobiotics, and a reduction in R-cells further impacted the absorption and storage of nutrients as well as other physiological activities including detoxification. Bautista et al. (2010) pointed out that the thickening of the cell membrane was ascribed to coagulation and obstruction of collagen fibres, melanin or haemocytes. Notably, vacuolation of epithelial cells was

observed after both Cd exposure and subsequent elimination (Fig. 2 c3, c4, c5 and c7). Beeby and Hopkin (1990) indicated that cells stored HM in vacuoles to reduce their metabolic availability. Excessive utilisation of accumulated saccharides and lipids is also responsible for vacuolation, which is regarded as a typical phenomenon of active detoxification (Sharma and Jindal 2020). The lesions observed in the present study and previous researches could cause severe dysfunctions and other physiological problems in individuals, ultimately led to death. Of course, the histopathological alternations seen in *S. henanense* appeared to be also the results of protection against Cd stress. As Mallatt and Sciences (1985) expressed, morphological changes are a kind of defence and adaptation for animals living in polluted environments.

The histopathological statistics were employed to quantify organs damage, which was convenient for the objectivity and accuracy of observations. This method has been used in several aquatic animals to directly reveal structural injuries, such as in fishes *Carassius auratus*, *Danio rerio* (Diniz et al. 2013) and *Catla catla* (Sharma and Jindal 2020), and the prawn *Macrobrachim potiuna* (de Melo et al. 2019). Almost all lesions of the gills in *S. henanense* were reversible, and I_{his} of the treatment groups were at a baseline level in the Cd-free water (Fig. 2 b). Rapid recovery of gill structures was directly associated with the high Cd elimination ability of the gills. Similarly, Guzmán-Guillén et al. (2017) reported that recovery of the gills in the fish *Oreochromis niloticu* exposed to 10 $\mu g \cdot L^{-1}$ cylindrospermopsin for 7 d was faster than that of liver, kidney and heart during 7 d of depuration. These findings further confirmed the significance of gills to aquatic animals, from the perspective of biological detoxification. Further, the development of hepatic tubules in *S. henanense* was normal, and the cells types were distinguishable during the depuration (Fig. 2 a5, a6). The I_{his} of TG1 and TG2 were the same as control at 28^{th} d, but the I_{his} of the hepatopancreas of crabs exposed to 500 $\mu g \cdot L^{-1}$ Cd still need a longer depuration to lower down (Fig. 2 d), which was in line with the ability of hepatopancreas in Cd sequestration. Similar results were also seen in the zebrafish *Danio rerio* exposed to 10 $mg \cdot L^{-1}$ TiO_2 nanoparticles for 14 d (Diniz et al. 2013), and the shrimp *Palaemonetes argentinus* exposed to 3.06 $\mu g\ L^{-1}$ Cd for 15 d (Chiodi Boudet et al. 2015). Yet the hepatopancreas did not recover completely when the zebrafish and shrimp were exposed to higher Cd concentrations. However, the recovery of the gills and hepatopancreas in *S. henanense* should be evaluated further with a prolonged period of Cd exposure.

Histochemistry, as a special technique contributed to clinical medicine, is not only used to display the damage of structure but also to locate and semi-quantify the changes of macromolecules. AB-PAS targeted carbohydrates and revealed neutral and acid polysaccharides of hepatopancreatic cells in *S. henanense* (Fig. 2 a1; Online Resource 3). Researches on the shrimp *Farfantepenaeus brasiliensis* (Nunes et al. 2014) and the prawn *Macrobrachium rosenbergii* (Silva et al. 2018) also reported similar abundance of polysaccharides storages in the hepatopancreas. In healthy *S. henanense*, the positive substances in the lumen may represent glycoproteins or waste released by B-cells because of the weak staining on the side near the proximal region of vacuoles in them. Also, these substances indicated the presence of mucus (mucins) which protected the tubular epithelium against mechanical pressure and pathogens (Silva et al. 2018). In *S. henanense*, Cd stress aggravated the secretions of B-cells, especially neutral polysaccharides (Fig. 2 a2). The strong staining of the plasma membrane of TG3 could be ascribed to the alterations of membrane structure caused by LPO or accelerated transcellular transport of neutral polysaccharides (Icelly and Nott 1992). Compared to the histochemical estimation of the hepatopancreas in the shrimp *Penaeus vannamei* (Cervellione et al. 2017) and the crab *Eriocheir sinensis* (Feng et al. 2019), the neutral lipids content was richer in *S. henanense* based on the ORO test (Fig. 2 b1; Online Resource 4). Lipids of the hepatopancreas in all treatment groups reduced and degraded (Fig. 2 b2; Table 2), contributing to the greater sensitivity of crabs to Cd toxicity. Using Sudan Black B detection, Schill and Köhler (2004) also found descended lipids of the hepatopancreas in the sow bug *Onsicus asellus* from long-term HM polluted soils. In most crustaceans, the hepatopancreas is the important site to store and metabolize carbohydrates and lipids (Vogt 2019), which meets the energy demand of physiological activities, such as molting (Li et al. 2017) and reproduction (Nunes et al. 2014), and assists the animals to overcome the harsh conditions such as starvation (Cervellione et al. 2017) and HM pollution (Schill and Köhler 2004). The abnormal DNA in the hepatopancreatic cells exposed to Cd was found when submitted to the Feulgen examination (Fig. 2 c2). *S. henanense* was able to save enough energy by apoptosis to overcome 50 $\mu g \cdot L^{-1}$ Cd exposure, and not completely cope with the high concentrations (TG2 and TG3), because most of the cells were necrotic (Online Resource 5). As shown in Fig. 2 d1-d3 and Online Resource 6, the protein granules in F- and B-cells were rich in hydrolases like trypsin and lipase, and those in R-cells stored nutrients (Icelly and Nott 1992). Moreover, two previous histochemical studies reported depleted protein of the liver in the catfish *Clarias gariepinus* (Sakr and Jamal Al Laial 2005) and the fish *Bagrus bayad* (Gaber et al. 2015) exposed to contaminants. However, no changes in the total proteins were seen in our research (Table 2), indicating the controllable proteolysis in crabs facing Cd stress.

During depuration, polysaccharides and neutral lipids of the hepatopancreas in *S. henanense* were restored (Fig. 2 a3, b3). As the maintenance costs reduced following the withdrawal of Cd, the growth and other activities of crabs would be promoted. For example, lipid accumulation is a desirable

signal, which shows the massive proliferation of liver cells or regeneration of the liver (Peng et al. 2018). Diniz et al. (2013) and Iheanacho and Odo (2020) also reported the recovery of carbohydrates and lipids of the liver in fishes *Danio rerio* and *Clarias gariepinus* in clean water following stress. The improved biological performance of *S. henanense* was partly attributed to the timely supply of diet during depuration. After all, fasting contributes to synergize Cd toxicity due to energy imbalance (Xue and Ke 2012). Hence, food shortage is one of the obstacles to self-repair of crabs in their natural habitats. As Kerambrun et al. (2014) stated, the storage of energy reserves in the fish *Scophthalmus maximus* would be compromised, if the food scarcity occurs during recovery following pollution events. The amplified DNA and damaged nuclear of epithelial cells returned to normal, which was before other biomacromolecules (Fig. 2 c3; Table 2). In terms of the present morphological results, the survivors in crabs were free from Cd threat, when transferred into a clean environment with favourable living conditions.

Oxidative stress will be triggered, when the bioavailable Cd beyond the detoxification threshold (Cuypers et al. 2010). Like mammals, aquatic animals are also equipped with an efficient antioxidative system against the redox imbalance (Aouini et al. 2018). SOD, CAT, GR and TrxR are widely employed in aquatic toxicological researches (Trevisan et al. 2011; Bakry et al. 2016; Zhang et al. 2019). Commonly, SOD-CAT system constitutes the first defence converting O_2^- to innocuous H_2O and O_2 (do Carmo et al. 2018), and GR and TrxR maintain the reduction of GSH and Trx to indirectly neutralize ROS (Ouyang et al. 2018). In the hepatopancreas of S. henanense, both of the correlations between SOD and TrxR (Table 3, $r = 0.909^*$), and those between CAT and GR (Table 3, $r = 0.847^*$) indicated the cooperation and interdependence between phase I and II metabolic enzymes to achieve comprehensive antioxidation (Otto and Moon 1996). The induced GR and TrxR activities are considered a protection against the oxidation of protein thiols, which maintain high GSH level and regenerated Trx (Trevisan et al. 2011). Jerome et al. (2017) explained the role of phase II metabolism, which catalysed the transformation of electrophilic compounds like transition-metals and MDA by conjugating reaction to prevent peroxidation effects. However, the gills of *S. henanense* showed significantly decreased SOD and TrxR activities ($p< 0.05$) when exposed to Cd (Table 4). Cadmium inhibits SOD activity by reducing the availability of bioelements, e.g., Fe, Mn, and Zn, which are components of SOD (Drąg-Kozak et al. 2019). Trevisan et al. (2014) also found the inhibited TrxR activity in Zn-exposed gills because of the combination of the divalent ions and the sulfhydryl groups. To reduce susceptibility to peroxidation, the gills of crabs showed a compensatory elevation of CAT and GR activities. The SOD and TrxR in *S. henanense* had the tissue-specificity responded to Cd exposure, signifying different ROS-quenching mechanisms in the gills and hepatopancreas. Despite limited knowledge with regards to GR and TrxR in crustaceans, but their role against poisons have been demonstrated in several aquatic animals, such as the mussel *Perna pernasnails* (Trevisan et al. 2014) and the snail *Biomphalaria alexandrina* (Bakry et al. 2016). Our data also suggest that GR and TrxR, the sulfhydryl-based enzymes, are interesting chemical parameters with prospective potential for antioxidant biomarkers in toxicological researches.

Upon Cd exposure, MDA content in crabs significantly increased ($p< 0.05$) (Table 4). Similar results caused by Cd were also found in the crab *Callinectes amnicola* (Jerome et al. 2017) and the crayfish *Procambarus clarkii* (Zhang et al. 2019). In our research, MDA level of the hepatopancreas increased but antioxidant enzymes were activated rather than depleted by ROS, which was ascribed to the higher content of polyunsaturated fatty acids or the need of more oxygen to detoxification (Pretto et al. 2010). The superfluous LPO increase the rigidity of plasma membrane, which affect the protection and communication of membrane (Dan et al. 2019). Apart from the cytopathological damage, physiological metabolism and transport of proteins and lipids are also interfered by unregulated LPO (Niki 2009). Moreover, the correlation analysis showed a positive association between I_{his} and MDA in *S. henanense* (Table 3, $r = 0.954^*$ in the gills, $r = 0.938^*$ in the hepatopancreas). In the carp *Catla catla*, the histopathological injuries of the liver, e.g., lymphocyte infiltration and karyolysis, were attributed to high MDA level (Sharma and Jindal 2020).

AChE, the key enzyme for the cholinergic system, is modified by HM (Harayashiki et al. 2016; Cheng et al. 2018; Chetoui et al. 2019), pesticides (Guilhermino et al. 2008; Ren et al. 2015; Ewere et al. 2019) and other contaminants. In the present study, two organs showed remarkably inhibited AChE activity ($p< 0.05$) after Cd exposure (Table 4). Metals are able to bind to the anionic portions of the cholinesterase molecule that affect the central nervous systems in aquatic invertebrates (Guilhermino et al. 2008). Branca et al. (2018) explained the neurotoxic mechanisms of Cd, including interference with neurotransmitter release and destruction of ACh receptors by competition with Ca^{2+}. Furthermore, we found a negative association between AChE and MDA (Table 3, $r = -0.876^*$ in the gills, $r = -0.771^*$ in the hepatopancreas) by Spearman's correlation coefficient. This potential relationship between neurotoxicity and oxidative stress was also coincided with Kim and Kang (2015) and Chetoui et al. (2019), who reported the neurotoxicity induced by redox imbalance.

During depuration, the SOD, CAT, GR, and TrxR activities of the gills recovered rapidly (Table 4), implying that the redox was in equilibrium again. Researches on the Pb-exposed fish *Platichthys stellatus* (Park et al. 2018) and the pharmaceuticals-exposed clam *Ruditapes philippinarum* (Trombini et al. 2019) also reported restored antioxidant

enzymes of the gills in a short period of purification. In contrast, *S. henanenses* showed later recovery of SOD, CAT, and TrxR activities of the hepatopancreas (Table 4), which verified its function of detoxification and biotransformation (Vogt 2019). Our findings agreed with Aouini et al. (2018), who studied the toxic effects and recovery of the clam *Ruditapes philippinarum* exposed to 10 and 100 $\mu g \cdot L^{-1}$ Pb for 7 d. Notably, GR activity of the hepatopancreas in *S. henanenses* was remarkably high ($p < 0.05$) even at the end of Cd elimination (Fig. 4 c2). Either activation or inactivation of antioxidant enzymes is considered an adaptation for stress disturbance, which may develop to new balance to acquire tolerance rather than return to the initial state when the stress removal (Dan et al. 2019). The MDA content and AChE activity in *S. henanenses* decreased to control after the withdrawal of Cd stress (Table 4), which was at least partly attributed to the excretion of Cd and a normal operation of antioxidant enzymes. The restored nutrient storages (Fig. 3 a3, b3) provided energy and materials, which also contributed to repair oxidative damage, such as degradation of useless proteins, base repairment, and re-synthesis of carbohydrates and lipids (Cuypers et al. 2010). Chiodi Boudet et al. (2015) and Dan et al. (2019) suggested that the recovery of MDA was a signal of redox balance in organisms. In our study, removal of neurotoxicity was easily achieved and with no tissue-specific (Table 4). Similar result was also published in the oysters *Saccostrea glomerate* after 4 d depuration following acute imidacloprid exposure (2 mg $\cdot L^{-1}$, 4 d) (Ewere et al. 2019). Pretto et al. (2010) indicated that aquatic species were able to increase the synthesis of AChE or decrease the release of Ach to regulate and maintain homeostasis of the nervous system. In short, *S. henanense* was able to detoxify within a relatively short depuration period of 21 d, as most biochemical and morphological biomarkers were normal and the Cd content in organs was also lowed.

Recently, the multiple-biomarkers instead of single biomarker have been employed to monitor environmental quality comprehensively and scientifically (Jerome et al. 2017). However, the information gained directly from different markers is messy and obscure. Given this, PCA is widely used to help estimate globally contaminants toxicity and analyse thoroughly the relationship between different biomarkers in the ecotoxicological studies (Arockia Vasanthi et al. 2014; Chetoui et al. 2019; Sharma and Jindal 2020). In our research, PCA aimed to identify and screen the most sensitive biomarkers in *S. henanense* at different experimental stages and different Cd concentrations in the presence and disappearance of stress. As shown in Fig. 5, under the low Cd bioaccumulation (TG1), the toxic response was organ-specific, i.e. the treated gills showed sensitive antioxidant defence but the hepatopancreas had only slight fluctuation in nerve conduction and hepatosomatic weight. By comparison, the TG2 and TG3 ellipses, which were characterized by high Cd bioaccumulation, redox imbalance and histopathological injuries, showed uniformity. Briefly, I_{his}, GR and MDA in the gills and hepatopancreas showed strong and specific responses ($p < 0.05$) from Cd exposure to depuration. They were used as the optimal biomarkers reflected the health conditions of crabs under the detoxification process.

Conclusions

We concluded that *S. henanense* resisted Cd toxicity by activating the antioxidant defence system and self-detoxify in clean environments. Compared with the hepatopancreas, the gills exhibited a better recovery and a higher ability to eliminate Cd. During depuration, structure and biomacromolecule injuries caused by Cd stress were able to be restored. A 21-d depuration period was regarded as a relatively short cycle of *S. henanense* to self-repair. Also, histopathological damage was more difficult to recover than biochemical damage. I_{his}, GR, and MDA could be employed as useful biomarkers indicating the health level of *S. henanense*. The elimination and detoxification as important factors should be considered in the study of ecotoxicology. Overall, our research documents the effects of Cd toxicity on the structure and function of the gills and hepatopancreas and complemented the detoxification to Cd in *S. henanense*. We provide new insights for optimizing the use of bioindicators in crustaceans for monitoring pollution and water quality in the freshwater ecosystem.

Supplementary Information The online version contains supplementary material available at https://doi.org/10.1007/s11356-021-14528-8.

Acknowledgements We want to allocate thanks to Dr. Xuelei Hu and Prof. Hans-Uwe Dahms for guidance in our research.

Author contribution L J, W E M and Z C Y performed sample collection of crabs. X Z H was a major operator of the experiment and contributor in writing the manuscript. All authors modified and approved the final manuscript.

Funding This study was funded by the National Natural Science Foundation of China (Grant No. 31672293), Shanxi Scholarship the Council of China (No. 2016-1), and the Shanxi Key Research and Development Program of China (No. 201703D221008-3).

Data availability The data and materials used or analyzed during the current study are available from the corresponding author on reasonable request.

Declarations

Ethics approval and consent to participate Not applicable

Consent for publication Not applicable

Competing interests The authors declare no competing interests.

References

Ahearn GA, Mandal PK, Mandal A (2004) Mechanisms of heavy-metal sequestration and detoxification in crustaceans: a review. J Comp Physiol B 174:439–452. https://doi.org/10.1007/s00360-004-0438-0

Aouini F, Trombini C, Volland M, Elcafsi M, Blasco J (2018) Assessing lead toxicity in the clam *Ruditapes philippinarum*: Bioaccumulation and biochemical responses. Ecotoxicol Environ Saf 158:193–203. https://doi.org/10.1016/j.ecoenv.2018.04.033

Arnér ES, Zhong L, Holmgren A (1999) Preparation and assay of mammalian thioredoxin and thioredoxin reductase. Methods Enzymol 300:226–239. https://doi.org/10.1016/s0076-6879(99)00129-9

Arockia Vasanthi L, Muruganandam A, Revathi P, Baskar B, Jayapriyan K, Baburajendran R, Munuswamy N (2014) The application of histo-cytopathological biomarkers in the mud crab *Scylla serrata* (Forskal) to assess heavy metal toxicity in Pulicat Lake, Chennai. Mar Pollut Bull 81:85–93. https://doi.org/10.1016/j.marpolbul.2014.02.016

Bakry FA, El-Hommossany K, Abd El-Atti M, Ismail SM (2016) Alterations in the fatty acid profile, antioxidant enzymes and protein pattern of *Biomphalaria alexandrina* snails exposed to the pesticides diazinon and profenfos. Toxicol Ind Health *32*:666–676. https://doi.org/10.1177/0748233713506770

Bartosz G (2009) Reactive oxygen species: destroyers or messengers? Biochem Pharmacol 77:1303–1315. https://doi.org/10.1016/j.bcp.2008.11.009

Bautista MN, Lavilla-Pitogo CR, Subosa PF, Begino ET (2010) Aflatoxin B1 contamination of shrimp feeds and its effect on growth and hepatopancreas of pre-adult *Penaeus monodon*. Agriculture 65:5–11. https://doi.org/10.1002/jsfa.2740650103

Beeby A, Hopkin SP (1990) Ecophysiology of Metals in Terrestrial Invertebrates. J Appl Ecol 27:762. https://doi.org/10.2307/2404325

Bernet D, Schmidt H, Meier W, Wahli T (1999) Histopathology in fish: proposal for a protocol to assess aquatic pollution. J Fish Dis 22:25–34

Bordon IC, Emerenciano AK, Melo JRC, Silva J, Favaro DIT, Gusso-Choueri PK, Campos BG, Abessa DMS (2018) Implications on the Pb bioaccumulation and metallothionein levels due to dietary and waterborne exposures: The *Callinectes danae* case. Ecotoxicol Environ Saf 162:415–422. https://doi.org/10.1016/j.ecoenv.2018.07.014

Bradford MM (1976) A rapid and sensitive method for the quantitation of microgram quantities of protein utilizing the principle of protein-dye binding. Anal Biochem 72:248–254. https://doi.org/10.1006/abio.1976.9999

Branca JJV, Morucci G, Pacini A (2018) Cadmium-induced neurotoxicity: still much ado. Neural Regen Res 13:1879–1882. https://doi.org/10.4103/1673-5374.239434

Cervellione F, McGurk C, Berger Eriksen T, Van den Broeck W (2017) Effect of starvation and refeeding on the hepatopancreas of whiteleg shrimp *Penaeus vannamei* (Boone) using computer-assisted image analysis. J Fish Dis 40:1707–1715. https://doi.org/10.1111/jfd.12639

Cheng L, Zhou JL, Cheng J (2018) Bioaccumulation, tissue distribution and joint toxicity of erythromycin and cadmium in Chinese mitten crab *Eriocheir sinensis*. Chemosphere 210:267–278. https://doi.org/10.1016/j.chemosphere.2018.07.005

Chetoui I, Bejaoui S, Trabelsi W, Rabeh I, Nechi S, Chelbi E, Ghalghaf M, El Cafsi M, Soudani N (2019) Exposure of *Mactra corallina* to acute doses of lead: effects on redox status, fatty acid composition and histomorphological aspect. Drug Chem Toxicol 22:1–13. https://doi.org/10.1080/01480545.2019.1693590

Chiodi Boudet LN, Polizzi P, Romero MB, Robles A, Marcovecchio JE, Gerpe MS (2015) Histopathological and biochemical evidence of hepatopancreatic toxicity caused by cadmium in white shrimp, *Palaemonetes argentinus*. Ecotoxicol Environ Saf 113:231–240. https://doi.org/10.1016/j.ecoenv.2014.11.019

Chiodi Boudet L, Mendieta J, Romero MB, Dolagaratz Carricavur A, Polizzi P, Marcovecchio JE, Gerpe M (2019) Strategies for cadmium detoxification in the white shrimp *Palaemon argentinus* from clean and polluted field locations. Chemosphere 236:124224. https://doi.org/10.1016/j.chemosphere.2019.06.194

Chubaka CE, Whiley H, Edwards JW, Ross KE (2018) Lead, Zinc, Copper, and Cadmium Content of Water from South Australian Rainwater Tanks. Int J Environ Res Public Health 15:1551. https://doi.org/10.3390/ijerph15071551

Cresswell T, Mazumder D, Callaghan PD, Nguyen A, Corry M, Simpson SL (2017) Metal Transfer among Organs Following Short- and Long-Term Exposure Using Autoradiography: Cadmium Bioaccumulation by the Freshwater Prawn *Macrobrachium australiense*. Environ Sci Technol 51:4054–4060. https://doi.org/10.1021/acs.est.6b06471

Cuypers A, Plusquin M, Remans T, Jozefczak M, Keunen E, Gielen H, Opdenakker K, Nair AR, Munters E, Artois TJ, Nawrot T, Vangronsveld J, Smeets K (2010) Cadmium stress: an oxidative challenge. Biometals 23:927–940. https://doi.org/10.1007/s10534-010-9329-x

Dan Z, Zhang X, Liu D, Ru S (2019) Cu accumulation, detoxification and tolerance in the red swamp crayfish *Procambarus clarkii*. Ecotoxicol Environ Saf 175:201–207. https://doi.org/10.1016/j.ecoenv.2019.03.031

de Melo MS, Dos Santos TPG, Jaramillo M, Nezzi L, Rauh Muller YM, Nazari EM (2019) Histopathological and ultrastructural indices for the assessment of glyphosate-based herbicide cytotoxicity in decapod crustacean hepatopancreas. Aquat Toxicol 210:207–214. https://doi.org/10.1016/j.aquatox.2019.03.007

Diniz MS, de Matos AP, Lourenço J, Castro L, Peres I, Mendonça E, Picado A (2013) Liver alterations in two freshwater fish species *Carassius auratus* and *Danio rerio* following exposure to different TiO_2 nanoparticle concentrations. Microsc Microanal 19:1131–1140. https://doi.org/10.1017/s1431927613013238

do Carmo T, Azevedo VC, de Siqueira PR, Galvão TD, Dos Santos FA, Dos Reis Martinez CB, Appoloni CR, Fernandes MN (2018) Reactive oxygen species and other biochemical and morphological biomarkers in the gills and kidneys of the Neotropical freshwater fish, *Prochilodus lineatus*, exposed to titanium dioxide (TiO_2) nanoparticles. Environ Sci Pollut Res Int 25:22963–22976. https://doi.org/10.1007/s11356-018-2393-4

Drąg-Kozak E, Pawlica-Gosiewska D, Gawlik K, Socha M, Gosiewski G, Łuszczek-Trojnar E, Solnica B, Popek W (2019) Cadmium-induced oxidative stress in Prussian carp (*Carassius gibelio* Bloch) hepatopancreas: ameliorating effect of melatonin. Environ Sci Pollut Res Int 26:12264–12279. https://doi.org/10.1007/s11356-019-04595-3

Duarte LFA, Moreno JB, Catharino MGM, Moreira EG, Trombini C, Pereira CDS (2019) Mangrove metal pollution induces biological tolerance to Cd on a crab sentinel species subpopulation. Sci Total Environ 687:768–779. https://doi.org/10.1016/j.scitotenv.2019.06.039

Ellman GL, Courtney KD, Andres VJ, Feather-Stone RM (1961) A new and rapid colorimetric determination of acetylcholinesterase activity. Biochem Pharmacol 7:88–95. https://doi.org/10.1016/0006-2952(61)90145-9

Ewere EE, Powell D, Rudd D, Reichelt-Brushett A, Mouatt P, Voelcker NH, Benkendorff K (2019) Uptake, depuration and sublethal effects of the neonicotinoid, imidacloprid, exposure in Sydney rock oysters. Chemosphere 230:1–13. https://doi.org/10.1016/j.chemosphere.2019.05.045

Feng D, Wang X, Li E, Bu X, Qiao F, Qin J, Chen L (2019) Dietary aroclor 1254-induced toxicity on antioxidant capacity, immunity

and energy metabolism in chinese mitten crab *Eriocheir sinensis*: amelioration by vitamin A. Front Physiol 10:722. https://doi.org/10.3389/fphys.2019.00722

Gaber HS, Ibrahim SA, El-Kasheif MA (2015) Histopathological and histochemical changes in the liver of *Bagrus bayad* caused by environmental pollution. Toxicol Ind Health 31:852–861. https://doi.org/10.1177/0748233713484653

Genchi G, Sinicropi MS, Lauria G, Carocci A, Catalano A (2020) The effects of cadmium toxicity. Int J Environ Res Public Health 17:3782. https://doi.org/10.3390/ijerph17113782

Guilhermino L, Barros P, Silva MC, Soares Amadeu MVM (2008) SHORT COMMUNICATION Should the use of inhibition of cholinesterases as a specific biomarker for organophosphate and carbamate pesticides be questioned. Biomarkers 3:157–163. https://doi.org/10.1080/135475098231318

Guzmán-Guillén R, Prieto Ortega AI, Moreno IM, Ríos V, Moyano R, Blanco A, Vasconcelos V, Cameán AM (2017) Effects of depuration on histopathological changes in tilapia *Oreochromis niloticus* after exposure to cylindrospermopsin. Environ Toxicol 32:1318–1332. https://doi.org/10.1002/tox.22326

Harayashiki CA, Reichelt-Brushett AJ, Liu L, Butcher P (2016) Behavioural and biochemical alterations in *Penaeus monodon* post-larvae diet-exposed to inorganic mercury. Chemosphere 164:241–247. https://doi.org/10.1016/j.chemosphere.2016.08.085

Hinton DE, Lauren DJ (1990) Integrative histopathological approaches to detecting effects of environmental stressors on fishes. Am Fish Soc Symp 8:51–66

Icelly J D, Nott J A (1992) Digestion and absorption: digestive system and associated organs, in: Harrison, F. W., Humes, A. G., (Eds), Microscopic Anatomy of Invertebrates. New York, pp. 147-201.

Iheanacho SC, Odo GE (2020) Dietary exposure to polyvinyl chloride microparticles induced oxidative stress and hepatic damage in *Clarias gariepinus* (Burchell, 1822). Environ Sci Pollut Res Int 27(17):21159–21173. https://doi.org/10.1007/s11356-020-08611-9

Jamwal A, Lemire D, Driessnack M, Naderi M, Niyogi S (2018) Interactive effects of chronic dietary selenomethionine and cadmium exposure in rainbow trout (*Oncorhynchus mykiss*): A preliminary study. Chemosphere 197:550–559. https://doi.org/10.1016/j.chemosphere.2018.01.087

Jerome FC, Hassan A, Omoniyi-Esan GO, Odujoko OO, Chukwuka AV (2017) Metal uptake, oxidative stress and histopathological alterations in gills and hepatopancreas of *Callinectes amnicola* exposed to industrial effluent. Ecotoxicol Environ Saf 139:179–193. https://doi.org/10.1016/j.ecoenv.2017.01.032

Jing W, Lang L, Lin Z, Liu N, Wang L (2019) Cadmium bioaccumulation and elimination in tissues of the freshwater mussel *Anodonta woodiana*. Chemosphere 219:321–327. https://doi.org/10.1016/j.chemosphere.2018.12.033

Johansson LH, Borg LA (1988) A spectrophotometric method for determination of catalase activity in small tissue samples. Anal Biochem 174:331–336. https://doi.org/10.1016/0003-2697(88)90554-4

Kasozi KI, Namubiru S, Kamugisha R, Eze ED, Tayebwa DS, Ssempijja F, Okpanachi AO, Kinyi HW, Atusiimirwe JK, Suubo J, Fernandez EM, Nshakira N, Tamale A (2019) Safety of Drinking Water from Primary Water Sources and Implications for the General Public in Uganda. J Environ Public Health 2019:7813962. https://doi.org/10.1155/2019/7813962

Kerambrun E, Henry F, Rabhi K, Amara R (2014) Effects of chemical stress and food limitation on the energy reserves and growth of turbot, *Scophthalmus maximus*. Environ Sci Pollut Res Int 21:13488–13495. https://doi.org/10.1007/s11356-014-3281-1

Kim JH, Kang JC (2015) Oxidative stress, neurotoxicity, and non-specific immune responses in juvenile red sea bream, *Pagrus major*, exposed to different waterborne selenium concentrations. Chemosphere 135:46–52. https://doi.org/10.1016/j.chemosphere.2015.03.062

Kubier A, Wilkin RT, Pichler T (2019) Cadmium in soils and groundwater: A review. Appl Geochem 108:1–16. https://doi.org/10.1016/j.apgeochem.2019.104388

Lee JW, Won EJ, Raisuddin S, Lee JS (2015) Significance of adverse outcome pathways in biomarker-based environmental risk assessment in aquatic organisms. J Environ Sci (China) 35:115–127. https://doi.org/10.1016/j.jes.2015.05.002

Lemus M, Salazar R, Lapo B, Chung K (2016) Metalotioneínas en bivalvos marinos. Lat Am J Aquat Res 44:202–215. https://doi.org/10.3856/vol44-issue2-fulltext-2

Li J, Li X, Wang L, Duan Q (2007) Advances in uptake, transportation and bioaccumulation of heavy metal ions in bivalves. Fish Sci 26:51e55

Li R, Zhu LN, Ren LQ, Weng JY, Sun JS (2017) Molecular cloning and characterization of glycogen synthase in *Eriocheir sinensis*. Comp Biochem Physiol B Biochem Mol Biol 214:47–56. https://doi.org/10.1016/j.cbpb.2017.09.004

Mallatt JJ, Sciences A (1985) Fish Gill Structural Changes Induced by Toxicants and Other Irritants: A Statistical Review. Can J Fish Aquat Sci 42:630–648

Mannervik B (2001) Measurement of glutathione reductase activity. Curr Protoc Toxicol Chapter 7 Unit 7.2. https://doi.org/10.1002/0471140856.tx0702s00.

Mansouri B, Maleki A, Davari B, Johari SA, Shahmoradi B, Mohammadi E, Shahsavari S (2016) Histopathological effects following short-term coexposure of *Cyprinus carpio* to nanoparticles of TiO2 and CuO. Environ Monit Assess 188:575. https://doi.org/10.1007/s10661-016-5579-6

Marsden ID, Rainbow PS (2004) Does the accumulation of trace metals in crustaceans affect their ecology—the amphipod example? J Exp Mar Biol Ecol 300:373–408

Negro CL, Collins P (2017) Histopathological effects of chlorpyrifos on the gills, hepatopancreas and gonads of the freshwater crab *Zilchiopsis collastinensis*. Persistent effects after exposure. Ecotoxicol Environ Saf 140:116–122. https://doi.org/10.1016/j.ecoenv.2017.02.030

Niki E (2009) Lipid peroxidation: physiological levels and dual biological effects. Free Radic Biol Med 47:469–484. https://doi.org/10.1016/j.freeradbiomed.2009.05.032

Nishikimi M (1975) Oxidation of ascorbic acid with superoxide anion generated by the xanthine-xanthine oxidase system. Biochem Biophys Res Commun 63:463–468. https://doi.org/10.1016/0006-291x(75)90710-x

Nunes ET, Braga AA, Camargo-Mathias MI (2014) Histochemical study of the hepatopancreas in adult females of the pink-shrimp *Farfantepenaeus brasiliensis Latreille*, 1817. Acta Histochem 116:243–251. https://doi.org/10.1016/j.acthis.2013.07.011

Ohkawa H, Ohishi N, Yagi K (1979) Assay for lipid peroxides in animal tissues by thiobarbituric acid reaction. Anal Biochem 95:351–358. https://doi.org/10.1016/0003-2697(79)90738-3

Otto DM, Moon TW (1996) Phase I and II enzymes and antioxidant responses in different tissues of brown bullheads from relatively polluted and non-polluted systems. Arch Environ Contam Toxicol 31:141–147. https://doi.org/10.1007/bf00203918

Ouyang Y, Peng Y, Li J, Holmgren A, Lu J (2018) Modulation of thiol-dependent redox system by metal ions via thioredoxin and glutaredoxin systems. Metallomics 10:218–228. https://doi.org/10.1039/c7mt00327g

Park HJ, Hwang IK, Kim KW, Kim JH, Kang JC (2018) Toxic effects and depuration on the antioxidant and neurotransmitter responses after dietary lead exposure in Starry Flounder. J Aquat Anim Health 30:245–252. https://doi.org/10.1002/aah.10033

Peng J, Yu J, Xu H, Kang C, Shaul PW, Guan Y, Zhang X, Su W (2018) Enhanced liver regeneration after partial hepatectomy in sterol regulatory element-binding protein (SREBP)-1c-Null Mice is Associated with Increased Hepatocellular Cholesterol Availability.

Cell Physiol Biochem 47:784–799. https://doi.org/10.1159/000490030

Pretto A, Loro VL, Morsch VM, Moraes BS, Menezes C, Clasen B, Hoehne L, Dressler V (2010) Acetylcholinesterase activity, lipid peroxidation, and bioaccumulation in silver catfish (*Rhamdia quelen*) exposed to cadmium. Arch Environ Contam Toxicol 58: 1008–1014. https://doi.org/10.1007/s00244-009-9419-3

Rainbow PS (2007) Trace metal bioaccumulation: models, metabolic availability and toxicity. Environ Int 33:576–582. https://doi.org/10.1016/j.envint.2006.05.007

Ren Z, Zhang X, Wang X, Qi P, Zhang B, Zeng Y, Fu R, Miao M (2015) AChE inhibition: one dominant factor for swimming behavior changes of *Daphnia magna* under DDVP exposure. Chemosphere 120:252–257. https://doi.org/10.1016/j.chemosphere.2014.06.081

Revathi P, Vasanthi LA, Munuswamy N (2011) Effect of cadmium on the ovarian development in the freshwater prawn *Macrobrachium rosenbergii* (De Man). Ecotoxicol Environ Saf 74:623–629. https://doi.org/10.1016/j.ecoenv.2010.08.027

Sakr SA, Jamal Al Laial SM (2005) Fenvalerate induced histopathological and histochemical changes in the liver of the catfish, *Clarias gariepinus*. J Appl Oral Sci 1:263–267

Salvat-Leal I, Verdiell D, Parrondo P, Barcala E, Romero D (2020) Assessing lead and cadmium pollution at the mouth of the river Segura using the invasive blue crab (*Callinectes sapidus*) as a bioindicator organism. Reg Stud Mar Sci 40:101521. https://doi.org/10.1016/j.rsma.2020.101521

Schill RO, Köhler HR (2004) Energy reserves and metal-storage granules in the hepatopancreas of *Oniscus asellus* and *Porcellio scaber* (Isopoda) from a metal gradient at Avonmouth, UK. Ecotoxicology 13:787–796. https://doi.org/10.1007/s10646-003-4476-2

Sharma R, Jindal R (2020) Assessment of cypermethrin induced hepatic toxicity in *Catla catla*: A multiple biomarker approach. Environ Res 184:109359. https://doi.org/10.1016/j.envres.2020.109359

Silva MAS, Almeida Neto ME, Ramiro BO, Santos ITF, Guerra RR (2018) Histomorphologic characterization of the hepatopancreas of freshwater prawn *Macrobrachium rosenbergii* (de man, 1879). Arq Bras Med Vet Zootec 70:1539–1546. https://doi.org/10.1590/1678-4162-10497

Singh R, Gautam N, Mishra A, Gupta R (2011) Heavy metals and living systems: An overview. Indian J Pharm 43:246–253. https://doi.org/10.4103/0253-7613.81505

Thévenod F (2010) Catch me if you can! Novel aspects of cadmium transport in mammalian cells. Biometals 23:857–875. https://doi.org/10.1007/s10534-010-9309-1

Trevisan R, Mello DF, Fisher AS, Schuwerack PM, Dafre AL, Moody AJ (2011) Selenium in water enhances antioxidant defenses and protects against copper-induced DNA damage in the blue mussel *Mytilus edulis*. Aquat Toxicol 101:64–71. https://doi.org/10.1016/j.aquatox.2010.09.003

Trevisan R, Mello DF, Uliano-Silva M, Delapedra G, Arl M, Dafre AL (2014) The biological importance of glutathione peroxidase and peroxiredoxin backup systems in bivalves during peroxide exposure. Mar Environ Res 101:81–90. https://doi.org/10.1016/j.marenvres.2014.09.004

Trombini C, Hampel M, Blasco J (2019) Assessing the effect of human pharmaceuticals (carbamazepine, diclofenac and ibuprofen) on the marine clam *Ruditapes philippinarum*: An integrative and multibiomarker approach. Aquat Toxicol 208:146–156. https://doi.org/10.1016/j.aquatox.2019.01.004

Viarengo A, Burlando B, Giordana A, Bolognesi C, Gabrielides GP (2000) Networking and expert-system analysis: next frontier in biomonitoring. Mar Environ Res 49:483–486. https://doi.org/10.1016/s0141-1136(00)00027-1

Vogt GJA (1987) Monitoring of environmental pollutants such as pesticides in prawn aquaculture by histological diagnosis. Aquaculture 67:157–164. https://doi.org/10.1016/0044-8486(87)90021-4

Vogt G (2019) Functional cytology of the hepatopancreas of decapod crustaceans. J Morphol 280:1405–1444. https://doi.org/10.1002/jmor.21040

Wiech M, Amlund H, Jensen KA, Aldenberg T, Duinker A, Maage A (2018) Tracing simultaneous cadmium accumulation from different uptake routes in brown crab *Cancer pagurus* by the use of stable isotopes. Aquat Toxicol 201:198–206. https://doi.org/10.1016/j.aquatox.2018.05.015

Xue M, Ke CH (2012) Cadmium bioaccumulation and its toxicity in *Babylonia areolata* under different nutritional status. J Appl Ecol 23:1965–1972 (in Chinese)

Zhang Y, Li Z, Kholodkevich S, Sharov A, Feng Y, Ren N, Sun K (2019) Cadmium-induced oxidative stress, histopathology, and transcriptome changes in the hepatopancreas of freshwater crayfish *Procambarus clarkii*. Sci Total Environ 666:944–955. https://doi.org/10.1016/j.scitotenv.2019.02.159

Zhao XM, Yao LA, Ma QL, Zhou GJ, Wang L, Fang QL, Xu ZC (2018) Distribution and ecological risk assessment of cadmium in water and sediment in Longjiang River, China: Implication on water quality management after pollution accident. Chemosphere 194:107–116. https://doi.org/10.1016/j.chemosphere.2017.11.127

Publisher's note Springer Nature remains neutral with regard to jurisdictional claims in published maps and institutional affiliations.